Supporting Information

E. coli-Based Semi-Artificial Photosynthesis: Biocompatibility of Redox Mediators and Electron Donors in [FeFe] Hydrogenase Driven Hydrogen Evolution

Mira T. Gamache[a,†], *Larissa Kurth*[a,†], *Dawit T. Filmon*[b], *Nicolas Plumeré*[b] *and Gustav Berggren*[a,*]

[a]Department of Chemistry - Ångström, Molecular Biomimetics, Uppsala University, Box 523, 75120 Uppsala, Sweden; E-mail: Gustav.berggren@kemi.uu.se

[b]TUM Campus Straubing for Biotechnology and Sustainability - Technical University of Munich, Uferstrasse 53, 94315 Straubing, Germany

† These authors contributed equally

Table of Contents

I. Experimental section

I.1. General

All chemicals were purchased from Sigma-Aldrich, Merck, and VWR, and used as received unless otherwise stated. All anaerobic work was performed in an MBRAUN glovebox under argon atmosphere.

I.2. Strains and plasmids

The expression vector and the gene coding for *Cr*HydA1 were kindly provided by Prof. Marc Fontecave (College de France, Paris/CEA, Grenoble). The gene encoding for Tam HydS was synthesized and cloned in pET-11a(+) by Genscript® using restriction sites NdeI and BamHI following codon optimization for expression in *E. coli*. The expression vector and the gene coding for CpI were kindly provided by Dr. Jifu Duan and Prof. Thomas Happe (Ruhr-Universität Bochum). The plasmids were used to transform the BL21(DE3) *E. coli* strain, which was used in the presented study.

I.3. Synthesis

The $[Fe_2(adt)(CO)_4(CN)_2](Et_4N)_2$ ($[2Fe]^{adt}$) complex was synthesized in accordance with literature protocols with minor modifications, and verified by FTIR spectroscopy.[1-4]

The diquat derivatives DQ-H and DQ-OH were synthesized according to procedures described in the literature (DQ-H[5], DQ-OH[6]). DQ-COOH (7-carboxy-3,11-dimethyl-7,8-dihydro-6H-dipyrido[1,2-a:2',1'-c][1,4]diazepine-5,9-diium) was synthesized according to the following procedure:

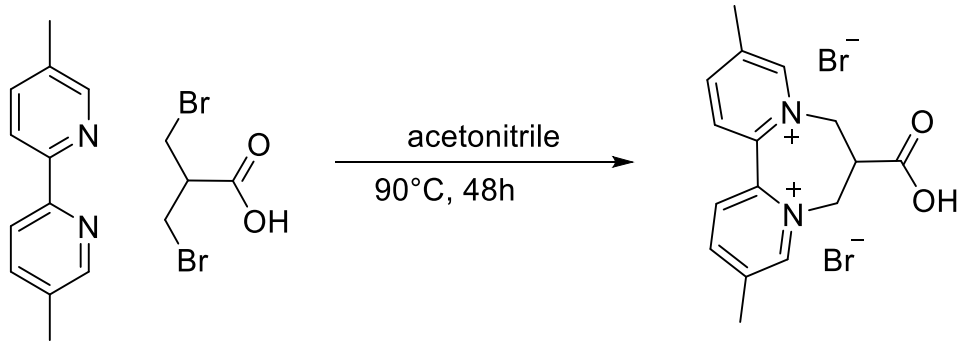

Scheme S.I. 1. Synthesis scheme of DQ-COOH.

5,5'-dimethyl-2,2'-bipyridine (1 g, 5,43 mmol) and 3-bromo-2-(bromomethyl)propanoic acid (4.22 g, 17.16 mmol) were dissolved in 8 ml acetonitrile in a flame-dried round-bottom flask, equipped with a stirrer. The mixture was refluxed at 90°C for 48h. The product was precipitated from diethyl ether and washed several times with ethyl acetate to obtain the product with a 87,7% yield.

^{1}H-NMR (400 MHz, D_2O): δ (H, ppm) = 9.22, 9.17 (d, 2H), 8.75 (s, 2H), 8.44, 8.41 (d, 2H), 5.38, 5.35 (m, 2H), 4.79, 4.71 (m, 2H), 4.34 (s, 1H), 2.73, 2.72 (s, 6H).

^{13}C-NMR (101 MHz, D_2O): δ (C, ppm) = 170.91, 148.63, 147.93, 143.67, 140.98, 131.18, 56.84, 56.30, 46.62, 18.22

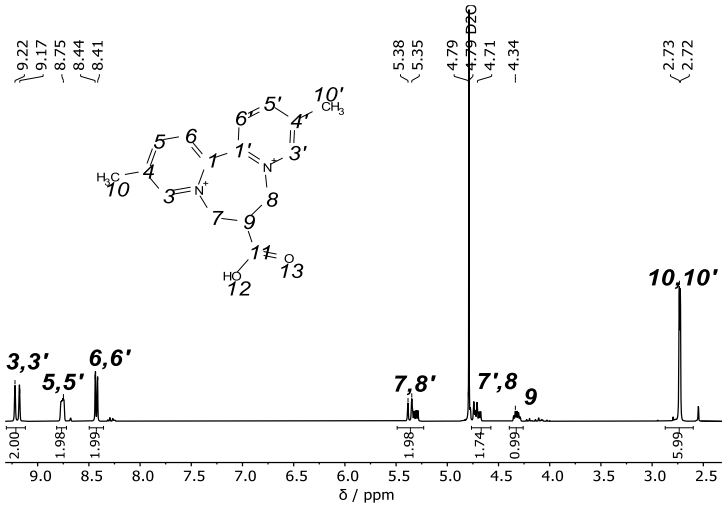

Figure S.I. 1. ^{1}H-NMR-spectrum of DQ-COOH recorded in D_2O. Chemical shifts are referenced to the signal of the solvent (δD_2O = 4.79 ppm)

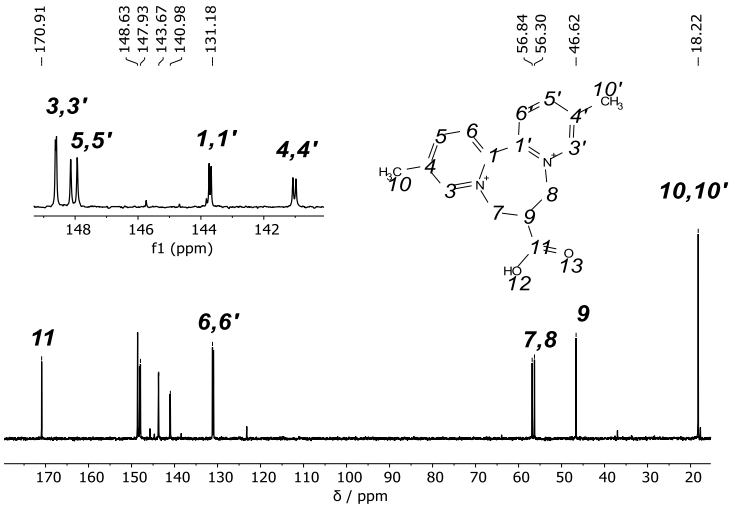

Figure S.I. 2. ^{13}C-NMR-spectrum of DQ-COOH recorded in D_2O.

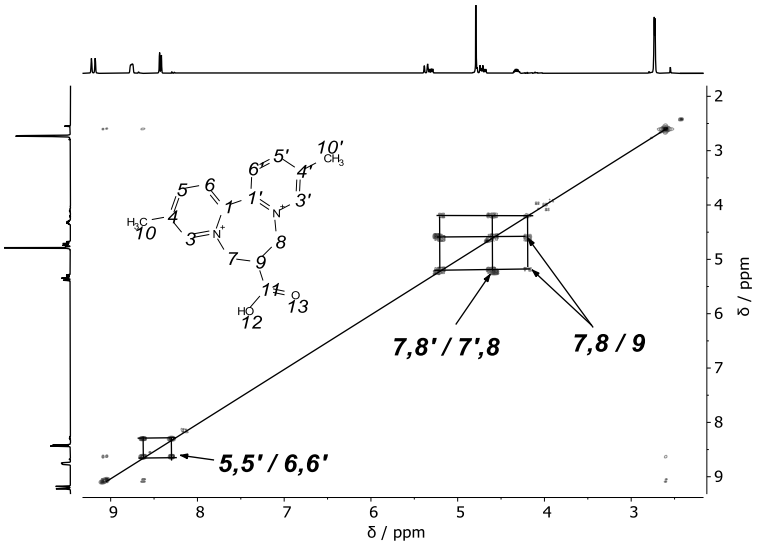

Figure S.I. 3. H,H-COSY-spectrum of DQ-COOH recorded in D_2O.

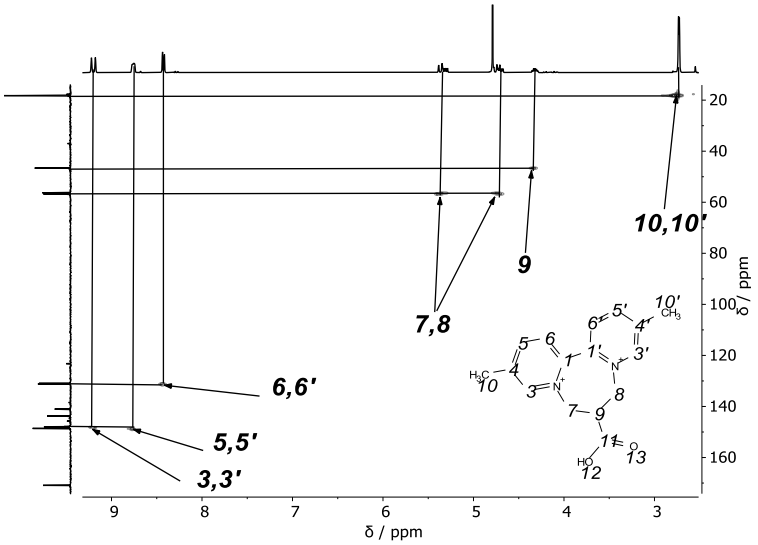

Figure S.I. 4. HSQC-spectrum of DQ-COOH recorded in D_2O.

I.4. Whole-cell sample preparation

Escheria coli whole-cell holo-*Cr*HydA1 samples were prepared as previously reported.[7] In short, cell cultures were grown in supplemented M9 media (70 mM phosphate buffer, 0.5 g/L NaCl, 1 g/L NH_4Cl, 1 mM $MgSO_4$, 100 µM $CaCl_2$, 4 g/L glucose, 100 µg/mL ampicilline) at 37 °C until the optical density at 600 nm was 0.6–0.8. The expression of the enzyme was induced by addition of IPTG (1 mM) and $FeSO_4$ (100 µM) at 20 °C for 14–16 hours. After washing, the cells are transferred into a glovebox and all subsequent steps are carried out under

anaerobic conditions. The cells are artificially matured by addition of $[2Fe]^{adt}$ (80 µM) for 1 h at 37 °C. The artificially matured cell suspensions were washed three times in Tris-HCl buffer supplemented with 150 mM NaCl (pH 8). The washed cells were then suspended in phosphate buffered saline (PBS, 100 mM NaH_2PO_4/Na_2HPO_4 with 150 mM NaCl, pH 6.5 or 7.5), supplemented with 100 mM of a sacrificial electron donor (SED), to yield an OD_{600} of 50.

Photocatalytic assays were prepared by taking 100 µL of the cell suspension, adding 16.7 µL of photosensitizer (PS, 6 mM) in PBS, redox mediator (RM, 10–20 mM) in PBS to yield a final concentration of 1 mM, and diluting to 1 mL final volume with PBS, supplemented with SED (100 mM, 200 mM or 500 mM as stated). This procedure yields a specific cell density OD_{600} of 5, a photosensitizer concentration of 100 µM, a RM concentration of 1 mM, and a SED concentration in the final sample of 90–100 mM.

Samples using TamHydS or CpI were prepared analogously, using the respective transformed cells.

I.5. Photocatalytic assays

Whole-cell samples (1 mL sample volume) were prepared in SureSTART™ glass vials (total volume 8 mL) and sealed with crimp cap and a rubber septum. The vials were placed on a shaker at 30 °C in the dark for 30 min. They were subsequently placed under a triphosphor fluorescent white lamp (Aura long life universal, 58W/865, 4000 lx, main emission 400–650 nm, see Figure S.I. 5) and kept under constant irradiation at 30 °C.

Hydrogen production was quantified by gas chromatography (PerkinElmer LLC, MA, USA) equipped with a thermal conductivity detector (TCD) and a stainless-steel column packed with molecular sieve (60/80 mesh). The operational temperatures of the injection port, the oven, and the detector were 100 °C, 80 °C and 100 °C, respectively. Argon was used as carrier gas at a flow rate of 35 mL min^{-1} and nitrogen as a reference gas.

The headspace of each sample was manually sampled by taking out 50 µL or 100 µL of the headspace volume with a gas-tight syringe. The amount of H_2 present in the headspace was estimated using a calibration curve (see below). Each reported sample was carried out in at least two biological replicates and at least two technical replicates each.

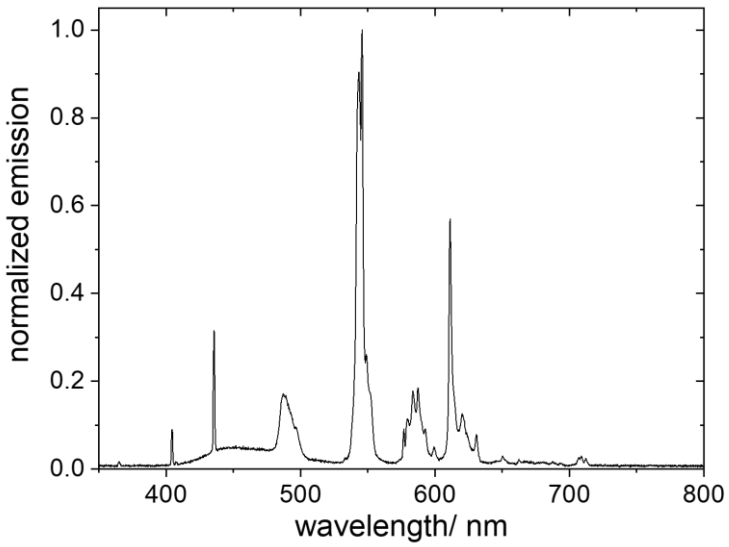

Figure S.I. 5. **Lamp profile.** Normalized emission spectrum of the triphosphor fluorescent white lamp used in photocatalytic experiments.

I.5.1. Addition experiments

For addition experiments, solutions containing 1 mM PS, 10 mM RM or 1 M SED or combinations thereof were prepared in PBS buffer (pH 6.5 for cysteine samples, pH 7.5 for TEOA samples). The solutions were degassed and ~100 µL were added to the photocatalytic samples at indicated timepoints. The samples were then incubated in the dark at 30 °C for 30 minutes before starting light irradiation.

I.5.2. Buffer separation assays

Photocatalytic samples were taken at different timepoints as indicated and transferred into a glovebox. Under inert gas atmosphere, the vials were opened and the cell-suspension was centrifuged at 14 500 rpm for 5 minutes. The supernatant was removed and the cell pellet was subsequently resuspended in PBS buffer with 100 mM SED (L-cysteine at pH 6.5, or TEOA at pH 7.5), adding 16.7 µL of PS (6 mM) in PBS, MV (10–20 mM) in PBS to yield a final concentration of 1 mM, yielding a final total volume of 1 mL. This procedure yields the same PS, SED and RM concentrations as in the photocatalytic sample prepared from fresh cell suspension. The samples were then incubated in the dark at 30 °C for 30 minutes before starting light irradiation.

I.6. H_2 calibration curve

To convert the observed H_2 peaks into the actual amount of H_2 produced by the sample, a calibration curve was conducted. The vials used for the photocatalytic assays were filled with 1 mL PBS in the glovebox, sealed, and placed on shakers at 30 °C. Using a syringe, discrete volumes (10–1000 µL) were taken out of each vial and replaced with the same volume of pure hydrogen gas. The samples were then placed on the shaker for 10–20 minutes and 50 or 100 µL of the headspace volume were sampled via GC. Each hydrogen concentration was carried out in triplicates. The resulting data points as well as a linear fit are shown in Figure S.I. 6.

The observed hydrogen peak in the GC measurements was correlated to the amount of hydrogen present in the injected sample $n(H_2)$ using the Ideal Gas Equation:

$$\boldsymbol{n(H_2) = \frac{V_{inj}(H_2) \cdot p}{R \cdot T}}$$

with $V_{inj}(H_2)$ being the percentual injected volume of H_2, (atmospheric) pressure p, temperature T and the Ideal Gas Constant R. The calculated n(H2) then refers to a discrete value of the integral of the experimentally determined H_2-peak (A_c) in the gas chromatogram. Linear regression of a plot of A_c with the y-intercept being fixed to 0 assigned to $n(H_2)$ in nmol yields a calibration equation of the form

$$\boldsymbol{A_c = b \cdot n(H_2)}$$

whereby the herein obtained slope b 2 668.216 66 functions as conversion factor for attributing a raw integral value (A_c) to a discrete amount of H_2 in the injected headspace sample. The total amount of H2 produced by a sample can then be calculated by multiplying with a factor of 70, accounting for the total headspace volume:

$$\boldsymbol{n_{total}(H_2) = A_c \,/\, 2668.21666 \cdot 7\,mL \,/\, 0.1\,mL}$$

All hydrogen production values are calculated this way, hence representing the total amount of hydrogen produced by a 1 mL sample with a cell density of $OD_{600} = 5$.

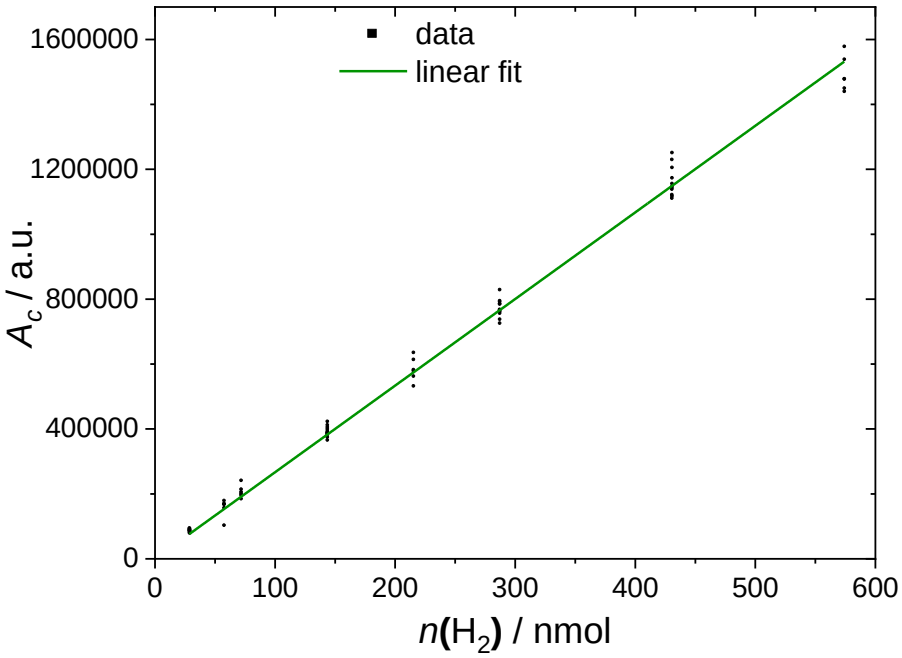

Figure S.I. 6**: H_2-Production Calibration Curve.** Calibration curve to examine the discrete amount of H_2 produced by photocatalytic samples via GC. The experimentally reported integral of the H_2-peak in gas chromatograms, A_c, is attributed to an amount of H_2 in nmol.

II. Photocatalytic assays

II.1. Different SEDs

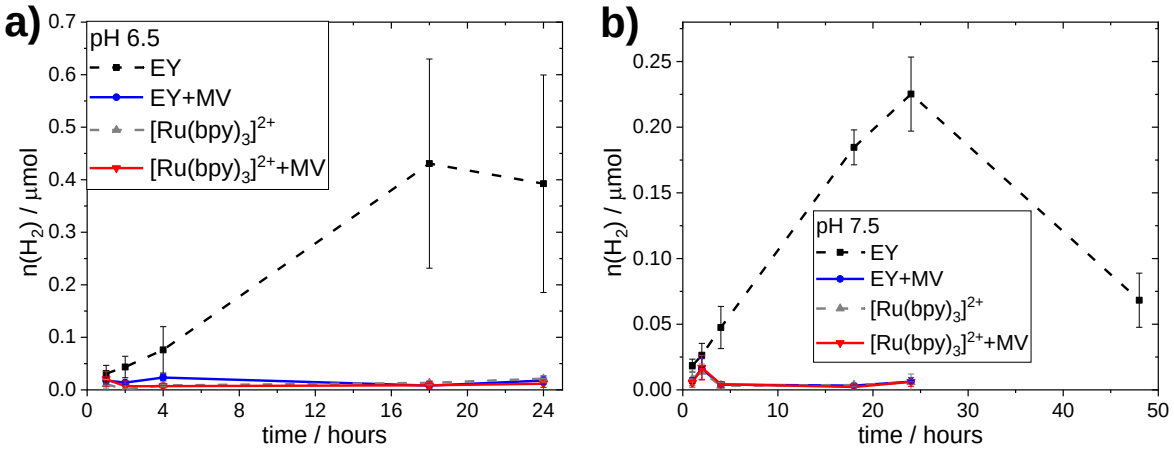

Figure S.I. 7. **Photocatalytic H_2-Production Assay with L-Ascorbic Acid**. Assays were performed in 100 mM PBS-buffer supplemented with 100 mM L-ascorbic acid, 100 µM PS (EY or $[Ru(bpy)_3]^2$), and 1 mM MV, carried out under inert gas atmosphere at 30 °C under continuous illumination. **a**: pH 6.5; **b**: pH 7.5.

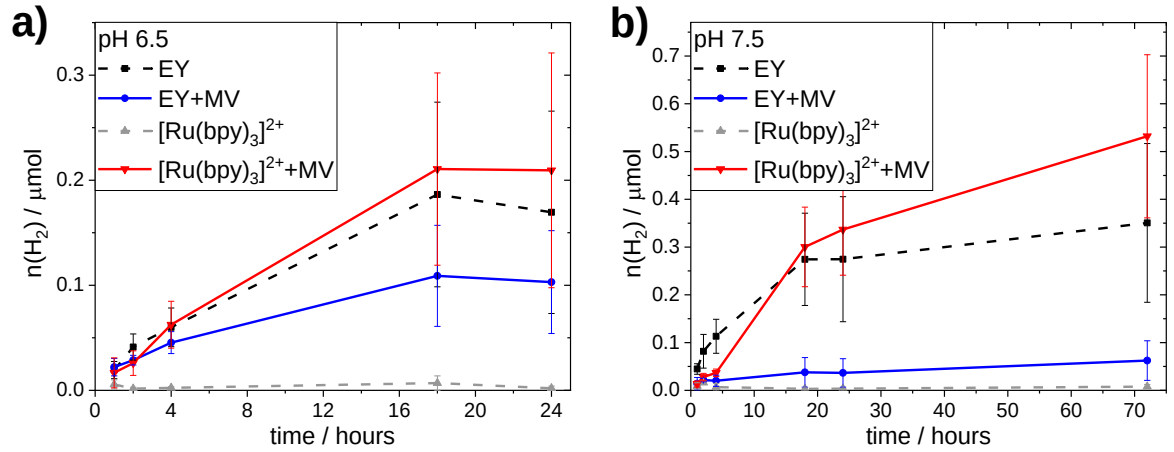

Figure S.I. 8. **Photocatalytic H_2-Production Assay with Lactic Acid.** Assays were performed in 100 mM PBS-buffer supplemented with 100 mM lactic acid, 100 µM PS (EY or $[Ru(bpy)_3]^{2+}$), and 1 mM MV, carried out under inert gas atmosphere at 30 °C under continuous illumination. **a**: pH 6.5 or **b**: pH 7.5 upon continuous illumination.

Generally, the H_2-production of these systems is low and the observed amounts of hydrogen production are not significantly above those observed for samples that lack an active hydrogenase, i.e. without the co-factor. This complicates a detailed analysis of the influence of the various photocatalytic components under these specific conditions.

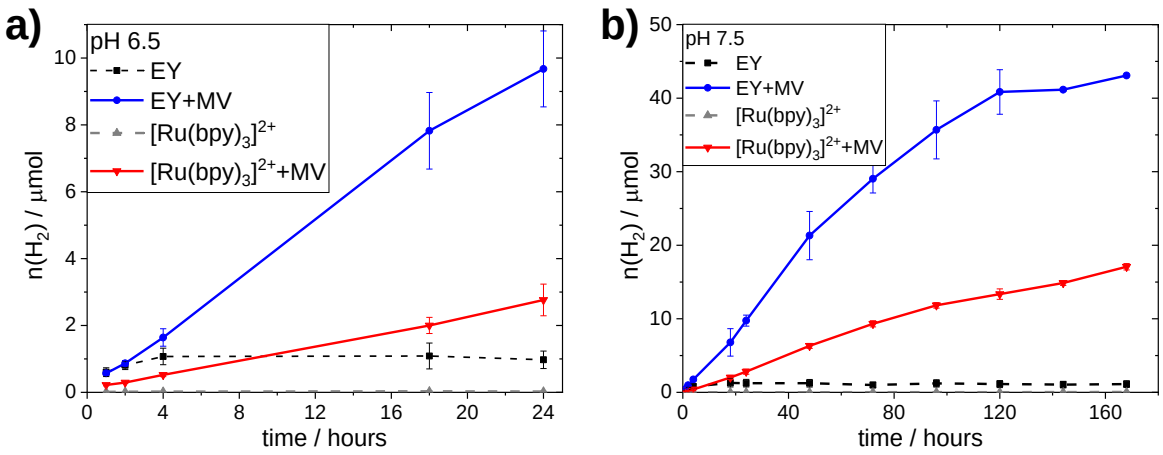

Figure S.I. 9. **Photocatalytic H_2-Production Assay with TEOA.** Assays were performed in 100 mM PBS-buffer supplemented with 100 mM TEOA, 100 µM PS (EY or $[Ru(bpy)_3]^{2+}$), and 1 mM MV, carried out under inert gas atmosphere at 30 °C under continuous illumination. **a**: pH 6.5 or **b**: pH 7.5 upon continuous illumination.

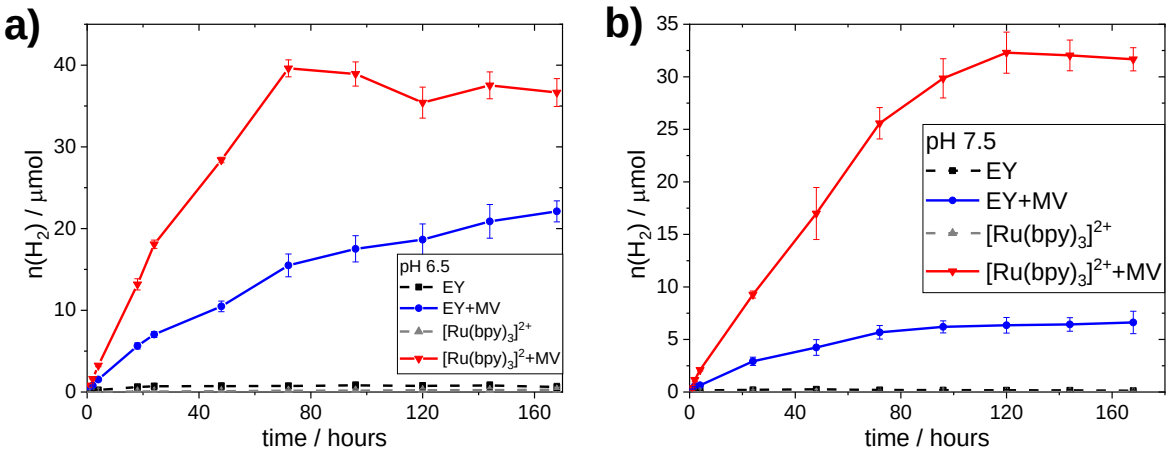

Figure S.I. 10. **Photocatalytic H_2-Production Assay with L-cysteine.** Assays were performed in 100 mM PBS-buffer supplemented with 100 mM L-cysteine, 100 µM PS (EY or $[Ru(bpy)_3]^{2+}$), and 1 mM MV, carried out under inert gas atmosphere at 30 °C under continuous illumination. **a**: pH 6.5 or **b**: pH 7.5 upon continuous illumination.

II.2. Different RMs

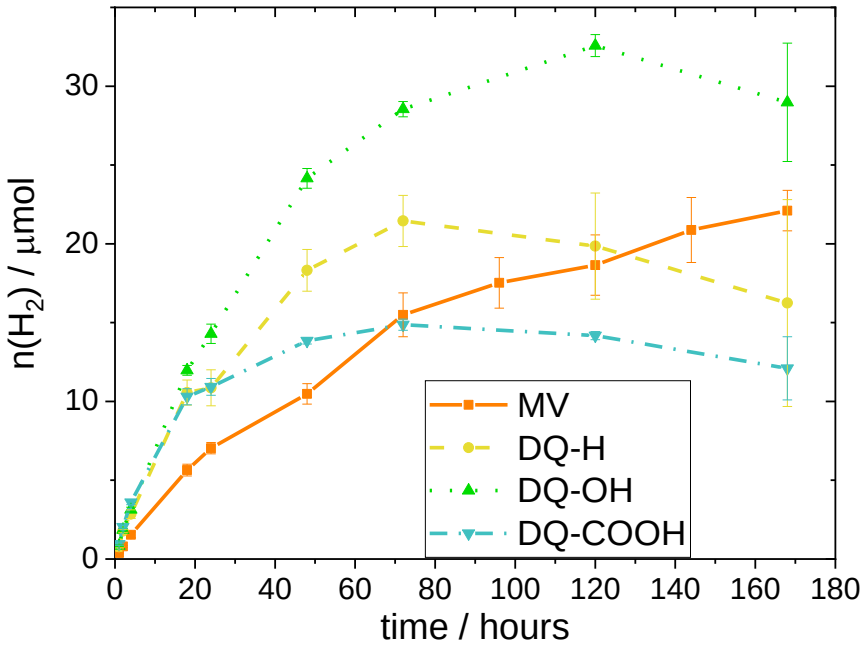

Figure S.I. 11. **Photocatalytic H_2-Production Assay with EY and Different RMs.** Assays were performed in 100 mM PBS-buffer (pH 6.5) supplemented with 100 mM L-cysteine, 100 µM EY, and 1 mM RM, carried out under inert gas atmosphere at 30 °C under continuous illumination (4000 lx).

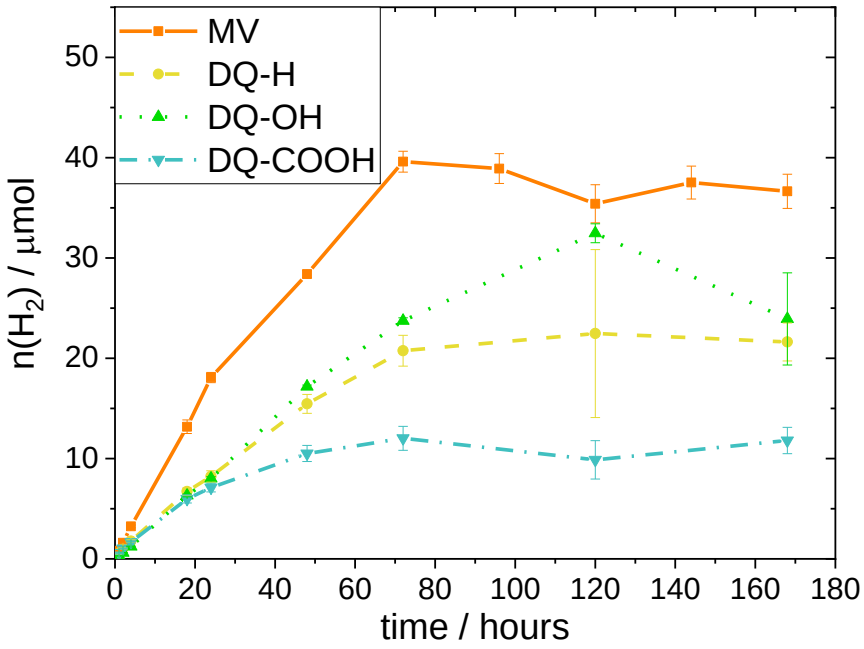

Figure S.I. 12. **Photocatalytic H_2-Production Assay with $[Ru(bpy)_3]^{2+}$ and Different RMs.** Assays were performed in 100 mM PBS-buffer (pH 6.5) supplemented with 100 mM L-cysteine, 100 µM $[Ru(bpy)_3]^{2+}$, and 1 mM RM, carried out under inert gas atmosphere at 30 °C under continuous illumination.

III. Cell viability studies

Cell viability studies were carried out by spreading cell suspension on agar plates. These plates were prepared with 20 g/L LB medium, and 100 mg/L ampicillin was added to each plate to select for *E. coli* cells harbouring the *Cr*HydA1 containing plasmid. The samples were prepared analogously to the photocatalytic samples and were kept under continuous irradiation at 30 °C. They were taken at different time points and 100 µL of the cell suspension was spread on the agar plates. The plates were incubated over night at 37 °C or over several days at room temperature. The cell growth was evaluated qualitatively by comparing the coverage of grown cells and putting each sample in one of five categories, which are shown in Figure S.I. 13 on representative examples. The results from these plating studies are summarized in Table 3 in the main manuscript.

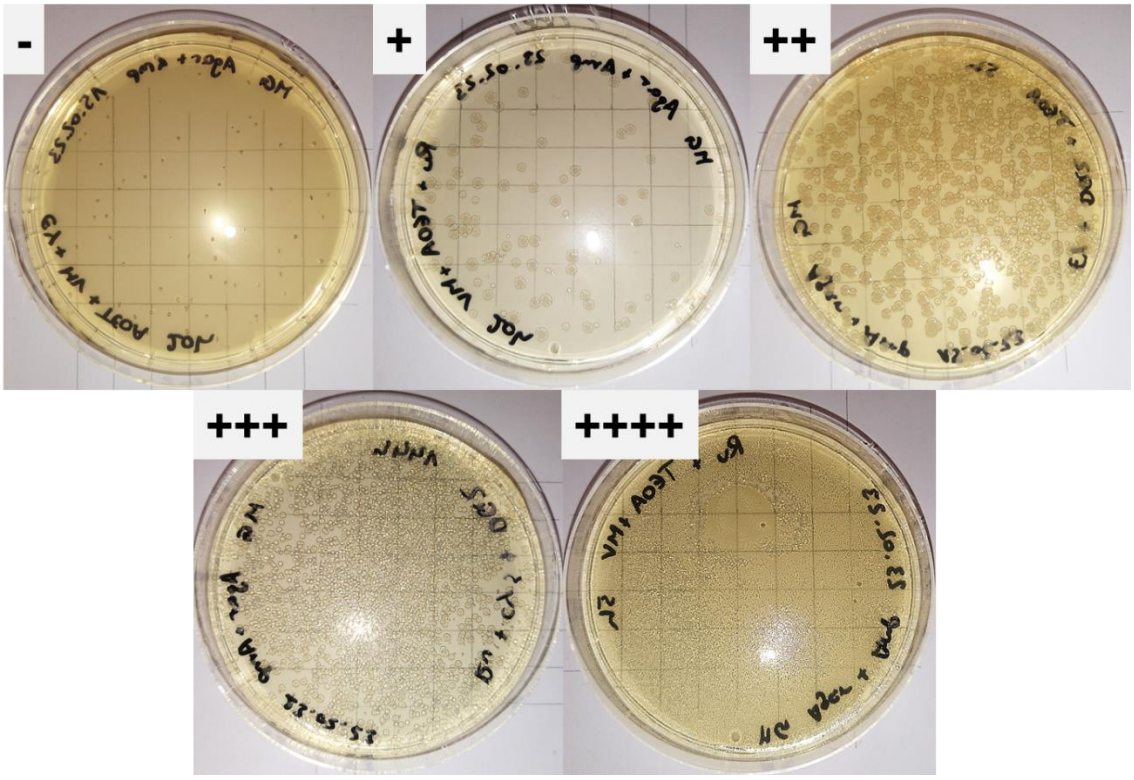

Figure S.I. 13. **Photographs of representative examples of plating experiments** corresponding to the different ratings in Table 3 of the main manuscript: – no cell growth (note that little dots stem from bubbles in the agar plate); + some well isolated cell colonies are observed; ++ usually well isolated cell colonies covering most of the plate; +++ most of the plate is covered in cell colonies; ++++ the plate is completely overgrown with no distinguishable cell colonies.

IV. Cyclic voltammetry of diquat derivatives

Electrochemical measurements were carried out under inert glovebox atmosphere using a three-electrode set-up with a glassy carbon electrode (3 mm diameter, CH Instruments), a graphite rod as counter electrode and an Ag/AgCl (1 M KCl) reference electrode (CH Instruments). Deoxygenated 100 mM PBS (pH 6.82) was used as electrolyte, with 2 mM (methyl viologen) or 1 mM (diquat derivatives) as analyte. Measurements were controlled by an Autolab PGSTAT10 potentiostat, with a scan rate of 50 mV/s and scan range of −0.5 V – −1.3 V vs Ag/AgCl (1 M KCl).

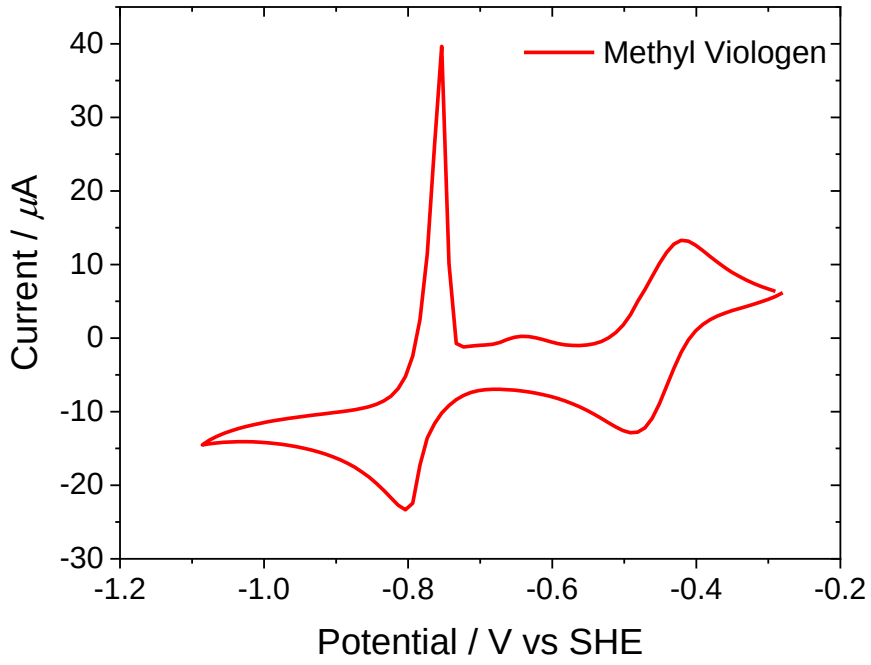

Figure S.I. 14. Cyclic voltammogram of MV (2 mM) in 100 mM PBS (pH = 6.82) under inert gas atmosphere; scan rate 50 mV/s.

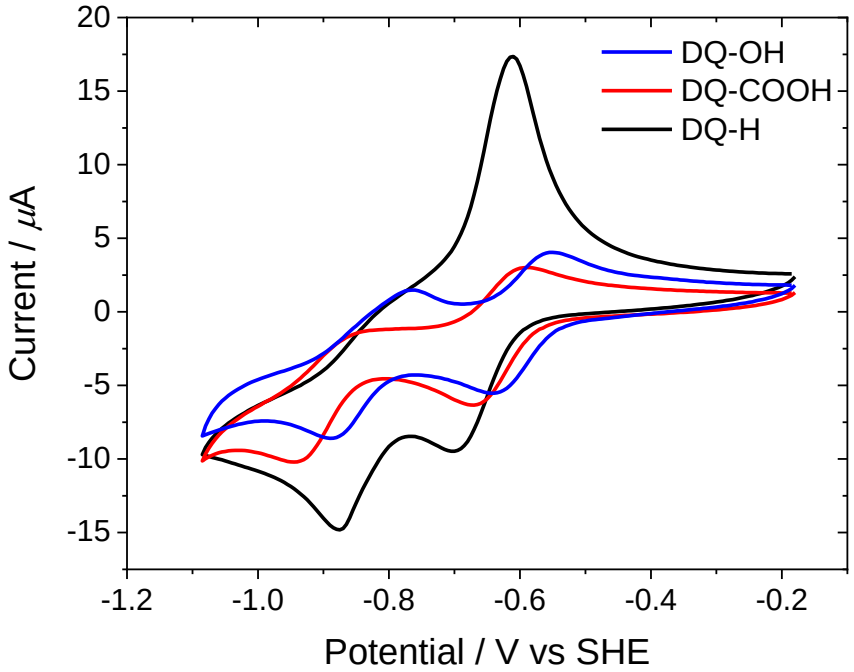

Figure S.I. 15. **Cyclic voltammogram of diquat derivatives** (1 mM) in 100 mM PBS (pH = 6.82) under inert gas atmosphere; scan rate 50 mV/s.

Table S.I. 1. Summary of the half-wave reduction potentials $E_{1/2}$ in V vs SHE of the first reduction of the redox mediators in PBS (pH = 6.82); peak separation ΔE_P in mV in brackets.

Redox mediator	**$E_{1/2}$ / V vs SHE (ΔE_P / mV)**
MV	-454 (70)
DQ-OH	-594 (85)
DQ-COOH	-633 (75)
DQ-H	-657 (90)

V. UV-vis absorption spectra of oxidized and reduced diquat derivatives

UV-vis absorption spectroscopy was carried out under inert glovebox atmosphere using an AvaSpec-ULS2048-USB2-UA-50: Avantes Fiber Optic UV/VIS/NIR spectrometer. Samples were prepared by dissolving each diquat derivative in 2.0 mL Tris-HCl buffer (1 M, pH 8), yielding a 5 mM stock solution. This solution was then diluted by a factor of 10, yielding 2.0 mL samples with a 50 µM concentration. Spectra were recorded in a 1 cm · 1 cm quartz glass cuvette.

Stock solutions of 20 mM $EuCl_2$ in Tris-HCl buffer (1 M, pH 8) as well as 20 mM ethylene glycol-bis(β-aminoethyl ether)-N,N,N′,N′-tetraacetic acid (EGTA) in Tris-HCl buffer (1 M, pH 8) were prepared. Upon equimolar mixing of these two solutions, $[Eu(EGTA)(H_2O)]^{2-}$ (20 mM) is formed in-situ.[8] This freshly prepared solution was then titrated to the diquat solution, mixed rigorously, and absorption spectra were recorded after each addition. Each titration was carried out two times. Maximal absorption of the reduced diquat derivatives was found at slight excess of $[Eu(EGTA)(H_2O)]^{2-}$.

The results are shown in Figure S.I. 16 and are summarized in Table S.I. 2.

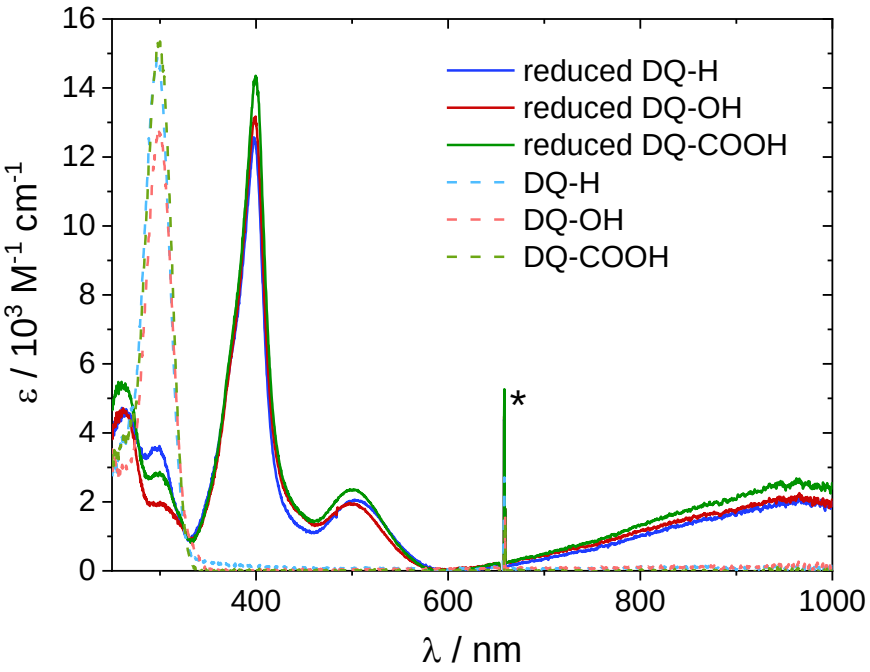

Figure S.I. 16. **UV-vis absorption spectra** of diquat derivatives in their oxidized and singly-reduced form; measurements carried out under inert-gas atmosphere in aqueous Tris-HCl buffer (1 M, pH 8). *artefact from lamp.

Table S.I. 2. Summary of absorption parameters of diquat derivatives in their oxidized state ($DQ\text{-}X^{2+}$) and their singly-reduced state ($DQ\text{-}X^{+}$).[a]

	absorption wavelength λ / nm (extinction coefficient ε / 10^3 M^{-1} cm^{-1})					
	$DQ\text{-}X^{2+}$	$DQ\text{-}X^{+}$				
DQ-H	297 (14.9)	265 (4.7)	299 (3.6)	399 (12.5)	504 (2.0)	965 (2.1)
DQ-OH	299 (12.7)	263 (4.6)	302 (1.9)	399 (13.1)	500 (1.9)	965 (2.2)
DQ-COOH	299 (15.3)	261 (5.3)	300 (2.8)	400 (14.4)	501 (2.3)	965 (2.6)

[a]maximum absorption wavelengths λ are reported in nm and extinction coefficients ε in 10^3 M^{-1} cm^{-1}; measurements carried out under inert-gas atmosphere in aqueous Tris-HCl buffer (1 M, pH 8).

VI. Transient absorption spectroscopy

VI.1. Nanosecond-laser pump probe transient absorption spectroscopy

The set-up has previously been described described.[9] The sample was excited using a Nd/YAG laser (Quantel, Brilliant) passed through an OPO tuned to 460 nm for experiments using $[Ru(bpy)_3]^{2+}$ and 516 nm for experiments using EY. The excitation energies varied from 14 to 17 mJ/pulse. The sample was probed using an unpulsed (for time-scales > 100 µs) or pulsed (for time-scales < 100 µs) Xe arc lamp perpendicular to the excitation light. The probe light was passed through one or two monochromators (Applied Photophysics, pbp Spectra Kinetic Monochromator 05-109) with one after the sample (2-mm slit opening) and an optional one before the sample (6-mm slit opening). The signal was detected using a photomultiplier tube (PMT, Hamamatsu R928), digitized using an oscilloscope (Agilent Technologies Infiniium 600 MHz) and processed using the Applied Photophysics LKS software. The measurements were carried out in 2 mm × 10 mm or 10 mm × 10 mm cuvettes, with the probe lamp passing through the 10 mm path in both cases.

All spectroscopic samples were prepared in a glovebox under anaerobic atmosphere in gas-tight cuvettes. Experiments are carried out in PBS solution (pH 6.5 or 7.5). The data is fitted with mono-exponential fit functions and reported values are an average of at least three individual traces. Representative traces are shown below and the results are summarized in Table S.I. 3, Scheme S.I. 2 and Scheme S.I. 3.

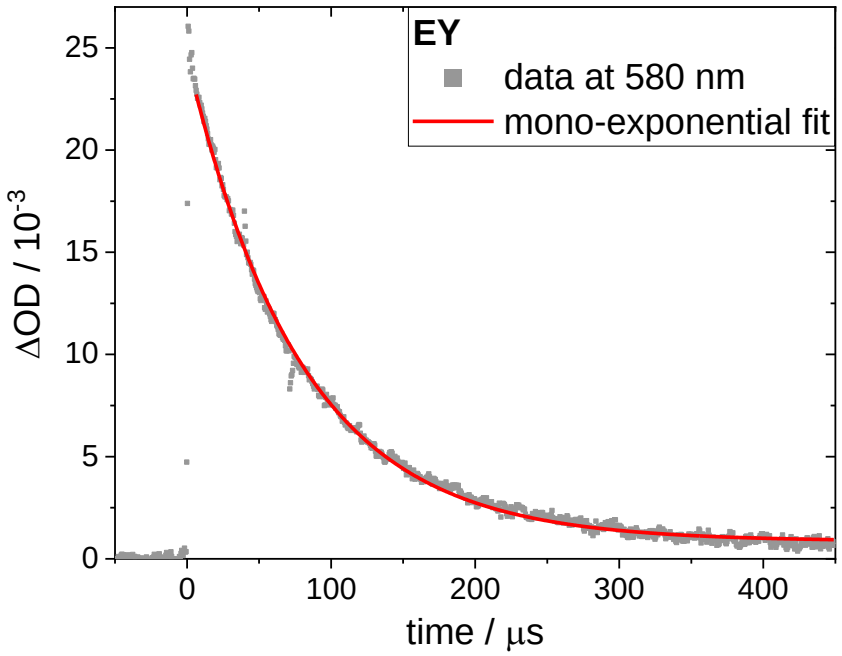

Figure S.I. 17. **Kinetic trace of absorption changes at 580 nm** (monitoring triplet excited-state absorption) of EY (4 µM) in PBS (pH 7.5) upon pulsed laser excitation at 516 nm; measurements conducted under inert gas atmosphere. Average rate constant: $(1.2\pm0.1)\cdot10^4$ s^{-1}.

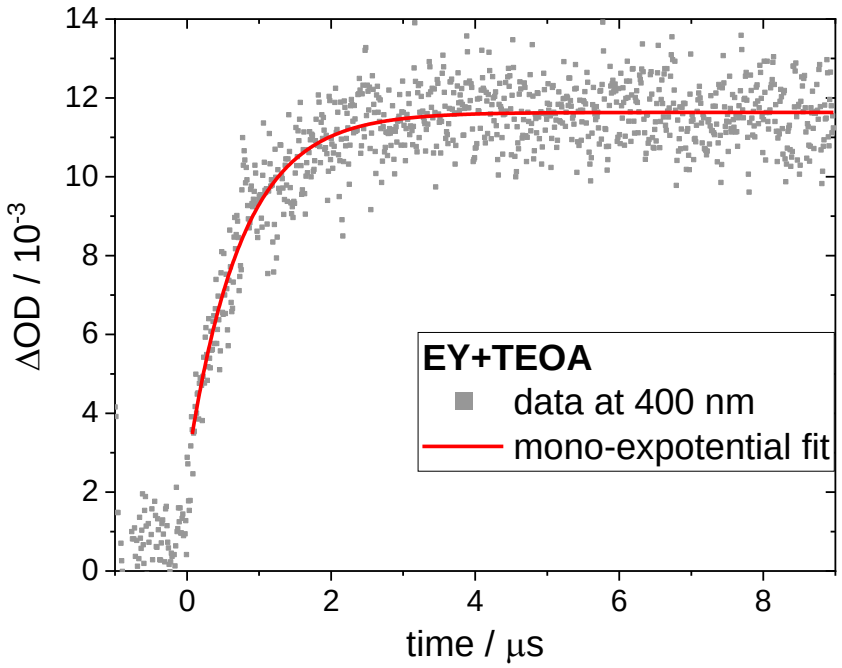

Figure S.I. 18. **Kinetic trace of absorption changes at 400** nm (monitoring reduced state absorption) of EY (4 µM) in the presence of TEOA (100 mM) in PBS (pH 7.5) upon pulsed laser excitation at 516 nm; measurements conducted under inert gas atmosphere. Average pseudo-first order rate constant: $(1.3\pm0.2)\cdot10^6$ s^{-1}. Average second order rate constant: $(1.3\pm0.2)\cdot10^7$ M^{-1} s^{-1}.

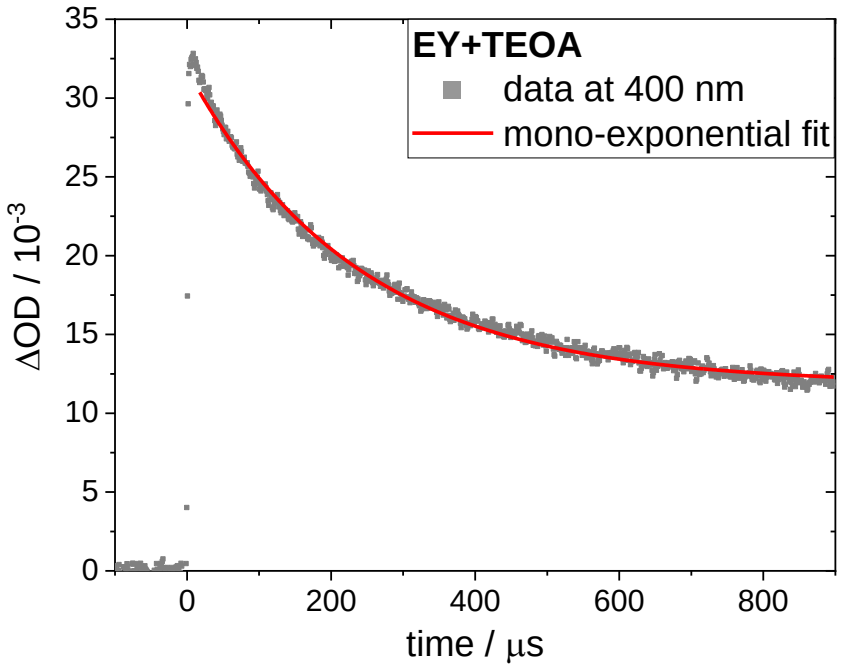

Figure S.I. 19. **Kinetic trace of absorption changes at 400** nm (monitoring reduced state absorption) of EY (4 μM) in the presence of TEOA (100 mM) in PBS (pH 7.5) upon pulsed laser excitation at 516 nm; measurements conducted under inert gas atmosphere. The observed decay corresponds to a multilayered degradation process of EY_{red} which is not complete at the shown timescale. Average observed first-order rate constant for decay: $(4.2\pm0.3)\cdot10^3$ s^{-1}.

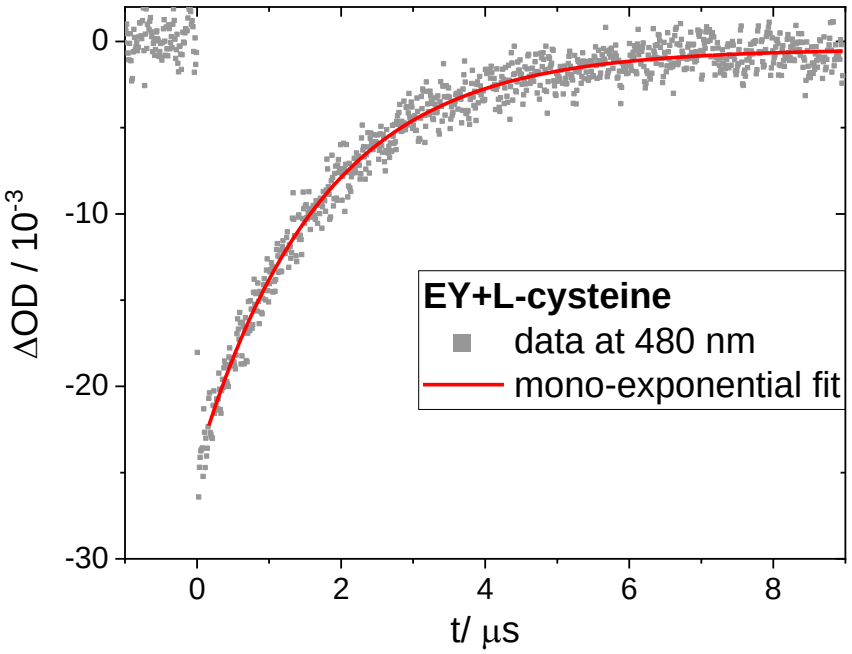

Figure S.I. 20. **Kinetic trace of absorption changes at 480 nm** (monitoring ground state bleach recovery) of EY (4 μM) in the presence of L-cysteine (100 mM) in PBS (pH 6.5) upon pulsed laser excitation at 516 nm; measurements conducted under inert gas atmosphere. Average pseudo-first order rate constant: $(5.8\pm0.5)\cdot10^{5}$ s^{-1}. Average second-order rate constant: $(5.7\pm0.5)\cdot10^{6}$ M^{-1} s^{-1}.

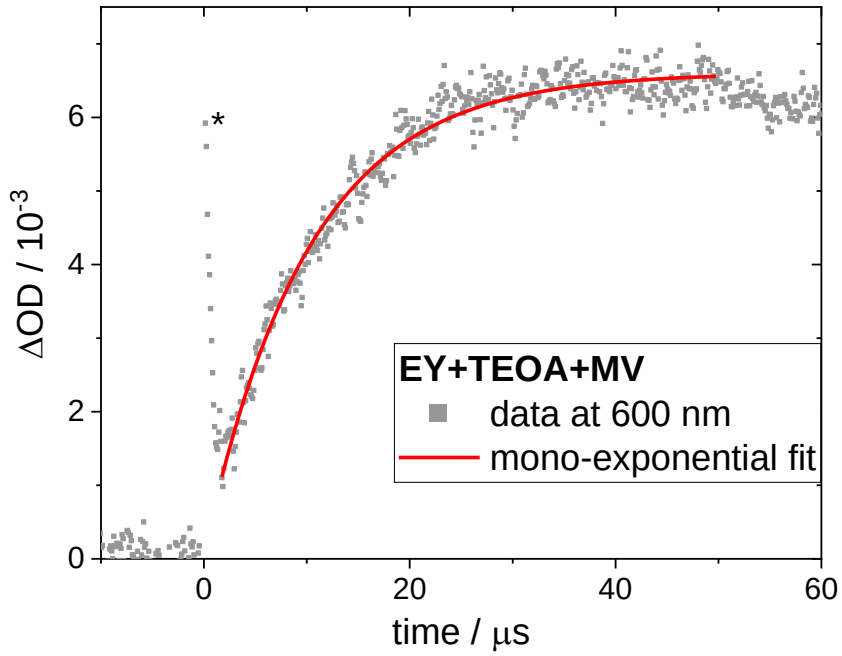

Figure S.I. 21. **Kinetic trace of absorption changes at 600 nm** (monitoring MV_{red} absorption) of EY (4 μM) in the presence of TEOA (100 mM) and MV (20 μM) in PBS (pH 7.5) upon pulsed laser excitation at 516 nm; measurements conducted under inert gas atmosphere. Average pseudo-first order rate constant: $(7.8\pm1.3)\cdot10^4$ s^{-1}. Average second-order rate constant: $(3.6\pm0.7)\cdot10^9$ M^{-1} s^{-1}. *at short time-scales a spike stemming from the excited-state absorption of EY can be observed.

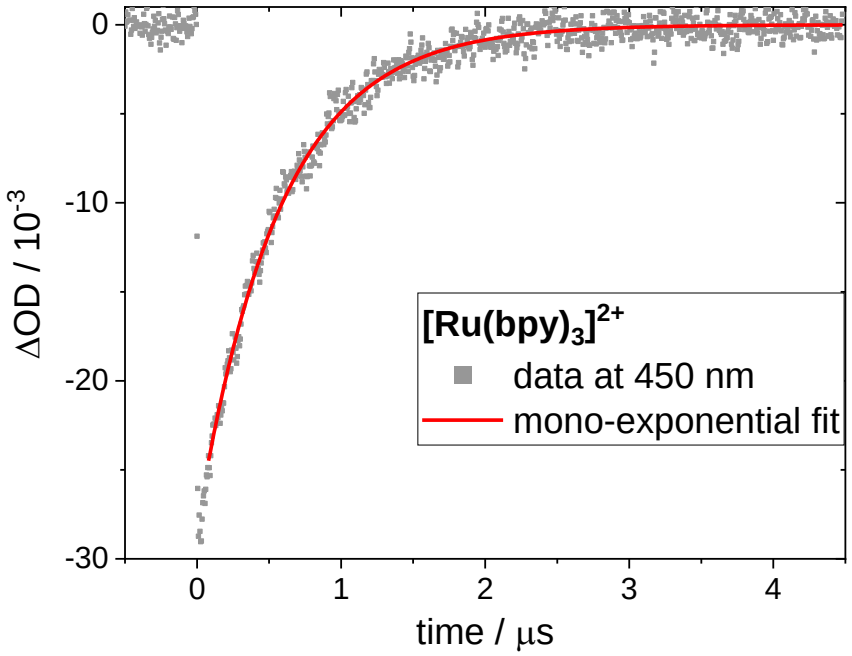

Figure S.I. 22. **Kinetic trace of absorption changes at 450 nm** (monitoring ground state bleach recovery) of $[Ru(bpy)_3]^{2+}$ (16 µM) in PBS (pH 6.5) upon pulsed laser excitation at 460 nm; measurements conducted under inert gas atmosphere. Average excited-state decay rate constant: $(1.76\pm0.05)\cdot10^6$ s^{-1}.

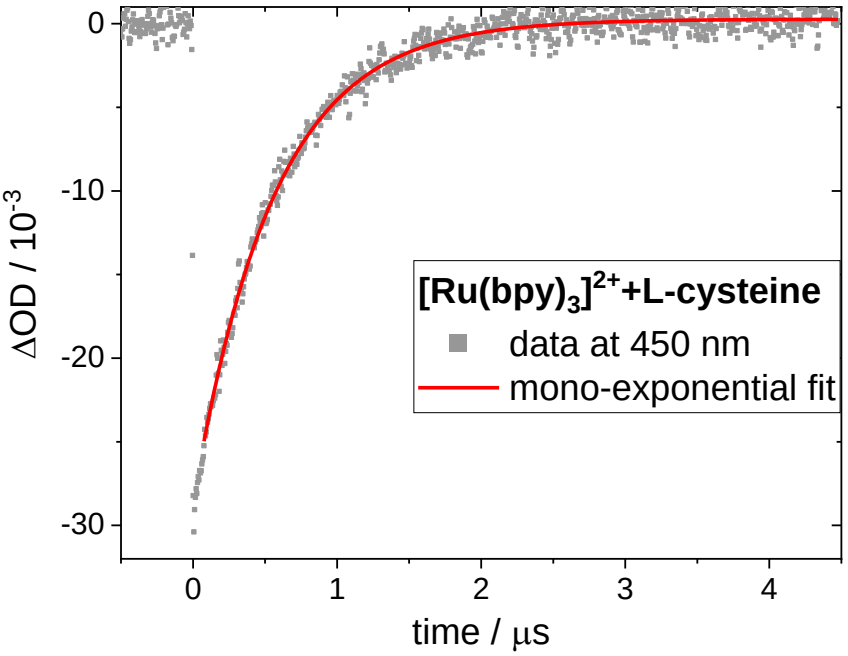

Figure S.I. 23. **Kinetic trace of absorption changes at 450 nm** (monitoring ground state bleach recovery) of $[Ru(bpy)_3]^{2+}$ (16 µM) in the presence of L-cysteine (100 mM) in PBS (pH 6.5) upon pulsed laser excitation at 460 nm; measurements conducted under inert gas atmosphere. Average observed rate constant: $(1.83\pm0.08)\cdot10^6$ s^{-1}.

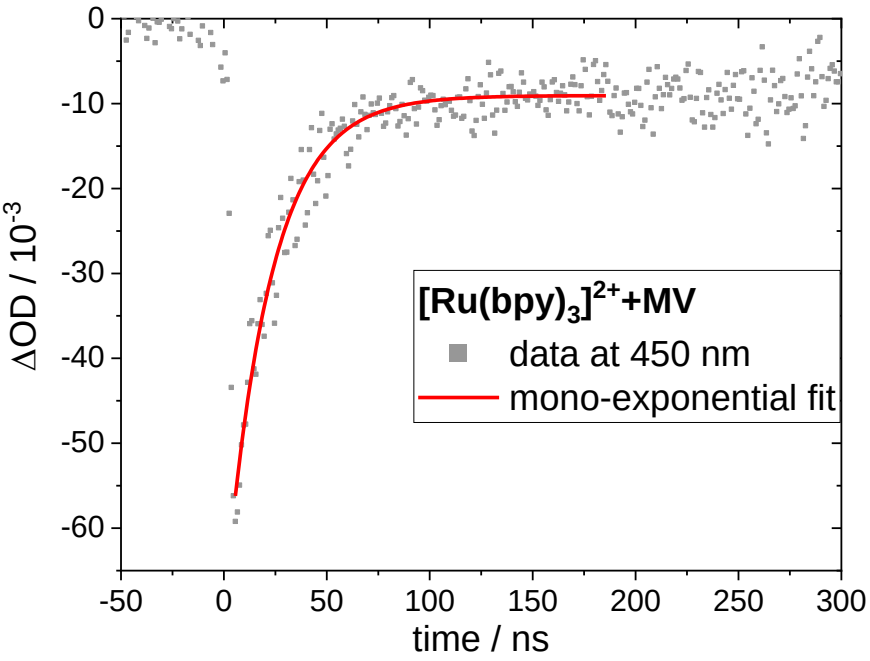

Figure S.I. 24. **Kinetic trace of absorption changes at 450 nm** (monitoring ground state bleach recovery) of $[Ru(bpy)_3]^{2+}$ (16 µM) in the presence of MV (30 mM) in PBS (pH 7.5) upon pulsed laser excitation at 460 nm; measurements conducted under inert gas atmosphere. Average observed rate constant: $(4.7\pm0.6)\cdot10^7$ s^{-1}. Average second order rate constant: $(1.5\pm0.3)\cdot10^9$ M^{-1} s^{-1}.

Literature values for the rate constant for the electron transfer from $[Ru(bpy)_3]^{2+}$* to MV in aqueous solution range between $5 \cdot 10^8$ M^{-1} s^{-1} and $5.6 \cdot 10^9$ M^{-1} s^{-1}.[10-16] These values are typically determined from quenching from the $[Ru(bpy)_3]^{2+}$* emission by MV.

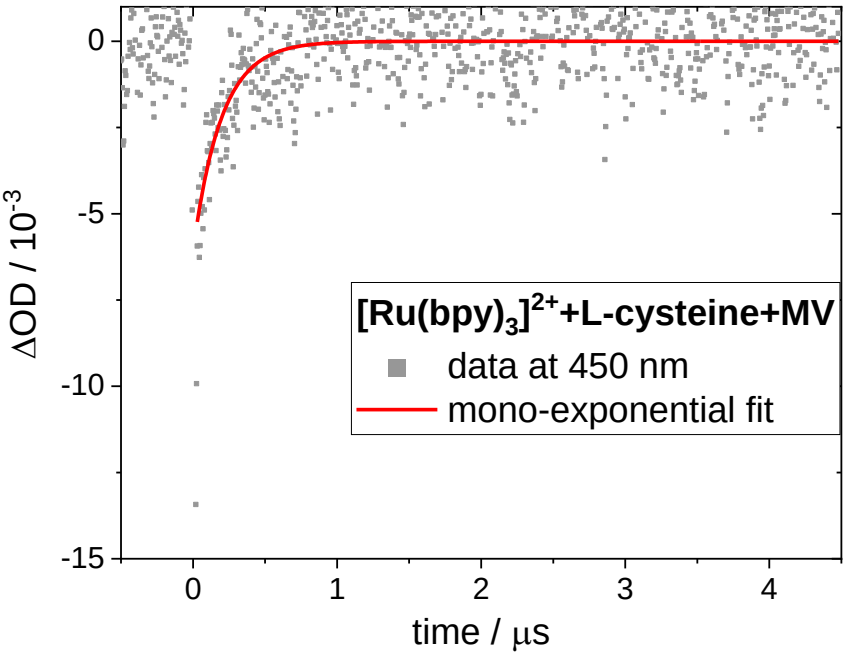

Figure S.I. 25. **Kinetic trace of absorption changes at 450 nm** (monitoring ground state bleach recovery) of $[Ru(bpy)_3]^{2+}$ (16 µM) in the presence of MV (30 mM) and L-cysteine (100 mM) in PBS (pH 6.5) upon pulsed laser excitation at 460 nm; measurements conducted under inert gas atmosphere. Average pseudo-first order rate constant: $(3.7 \pm 1.2) \cdot 10^6$ s^{-1}. Average second order rate constant: $(3.7 \pm 1.2) \cdot 10^7$ M^{-1} s^{-1}.

In the presence of different electron donors, a rate for photoreduction of MV by $[Ru(bpy)_3]^{2+}$* of $2.5 \cdot 10^8$ M^{-1} s^{-1} (with mercaptoethanol) to $2.9 \cdot 10^8$ M^{-1} s^{-1} (with TEOA) has been reported.[17] These values were gained by studying the formation of MV_{red} absorption bands. slightly ranging from $6.5 \cdot 10^6$ M^{-1} s^{-1} to have been reported.[10, 17]

Table S.I. 3. Summary of the rate constants reported in this study. Values are calculated from averages of the mono-exponential fits of at least three individual traces.

Reaction	**rate constant**
EY* → EY	$(1.2\pm0.1)\cdot10^{4}$ s^{-1}
EY* + TEOA → EY_{red} + $TEOA_{ox}$	$(1.3\pm0.2)\cdot10^{7}$ M^{-1} s^{-1}
[a]EY_{red} → decomposition products	$(4.2\pm0.3)\cdot10^{3}$ s^{-1}
EY* + L-cysteine → EY_{red}	$(5.7\pm0.5)\cdot10^{6}$ M^{-1} s^{-1}
EY_{red} + MV → EY + MV_{red}	$(3.6\pm0.7)\cdot10^{9}$ M^{-1} s^{-1}
$[Ru(bpy)_3]^{2+}$* → $[Ru(bpy)_3]^{2+}$	$(1.76\pm0.05)\cdot10^{6}$ s^{-1}
[a]$[Ru(bpy)_3]^{2+}$* + L-cysteine → $[Ru(bpy)_3]^{+}$ + $L\text{-cysteine}_{ox}$	$(1.83\pm0.08)\cdot10^{6}$ s^{-1}
$[Ru(bpy)_3]^{2+}$* + MV → $[Ru(bpy)_3]^{3+}$ + MV_{red}	$(1.5\pm0.3)\cdot10^{9}$ M^{-1} s^{-1}
$[Ru(bpy)_3]^{3+}$ + L-cysteine → $[Ru(bpy)_3]^{2+}$ + $L\text{-cysteine}_{ox}$	$(3.7\pm1.2)\cdot10^{7}$ M^{-1} s^{-1}

[a] pseudo-first order rate constant

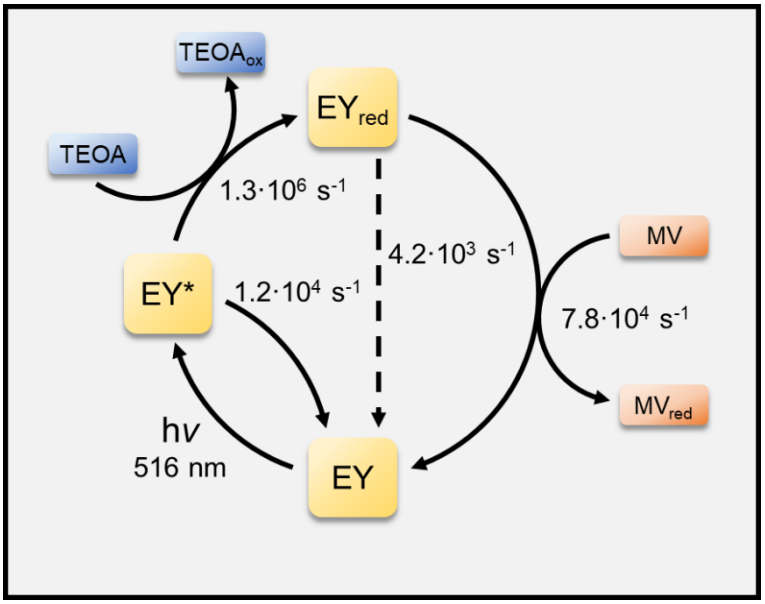

Scheme S.I. 2. **Schematic representation of the reductive quenching photocatalytic cycle** involving EY as photosensitizer (4 µM), TEOA as sacrificial electron donor (100 mM), and MV (20 µM), as electron acceptor; pseudo-first order rate constants as obtained by transient absorption spectroscopy. Reported values are averages of three or more individual traces.

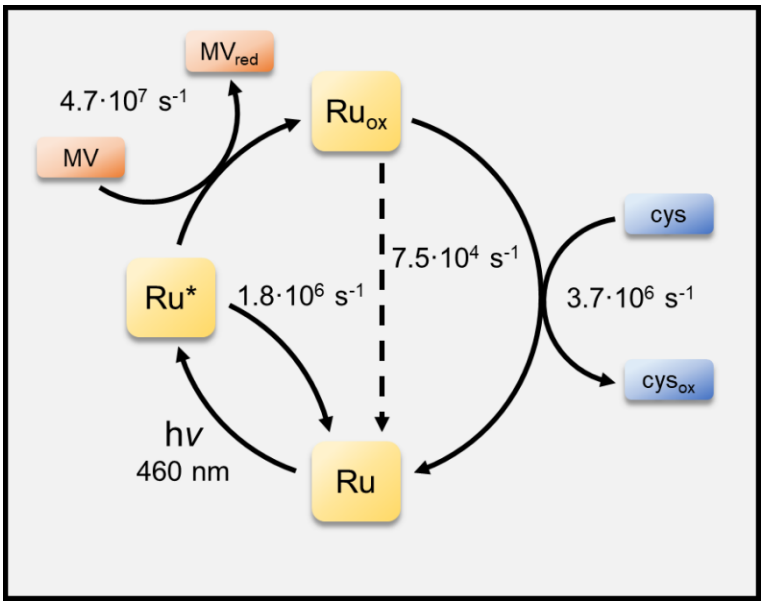

Scheme S.I. 3. **Schematic representation of the oxidative quenching photocatalytic cycle** involving $[Ru(bpy)_3]^{2+}$ (Ru) as photosensitizer (16 µM), L-cysteine (cys) as sacrificial electron donor (100 mM), and MV (30 mM), as electron acceptor; pseudo-first order rate constants as obtained by transient absorption spectroscopy. Reported values are averages of three or more individual traces.

VI.2. Reduced redox mediator accumulation

Experiments were carried out either on a Varian Cary 50 UV-Vis Spectrophotometer, using a 530 nm pulsed LED lamp for excitation, or an Agilent 8453 diode array UV–vis spectrometer, using a 447.5 nm LED (Luxeon Star, Rebel premounted LED fitted with carlco 29.8/10 mm lens) that was controlled by an HP 8116A 50 MHz pulse/function generator. In both set-ups, the LED was set to continuous illumination (447.5 nm LED)/ continuous pulsing (530 nm LED) and the accumulation of RM_{red} was followed by either the absorption at 400 nm (MV and DQ derivatives) or 600 nm (MV).

Samples contained 4 µM PS, 20–25 µM RM, 100 mM SED in PBS (pH 6.5 for samples with L-cysteine, pH 7.5 samples with TEOA). Samples were prepared under inert-gas atmosphere and experiments were carried out in 10x10 mm quartz glass cuvettes. For *in vivo* experiments, cell suspensions were prepared as described above (section I.4). The final OD_{600} was 0.17.

The solution potentials were calculated using the Nernst equation.

$$E = E_0 - RT/Fn \ ln[red/ox] \qquad (1)$$

with E_0 being the standard redox potential of the RM, R being the universal gas constant, T the temperature in Kelvin, F the Faraday constant, n the number of electrons transferred, *[red]* being the concentration of RM_{red} when a (pseudo) steady state is reached and *[ox]* being the concentration of remaining RM in solution. It should be noted that the solution potential cannot be directly correlated to the driving force of the electron transfer step from the RM to the cellular acceptor. Yet, it can act as a measure which combines thermodynamic driving force (i.e. the standard redox potential of the RM) and kinetic effects stemming from the different concentrations of RM_{red} present in the solution.

The results are summarized in Figure S.I. 26 and Table 2 in the main manuscript.

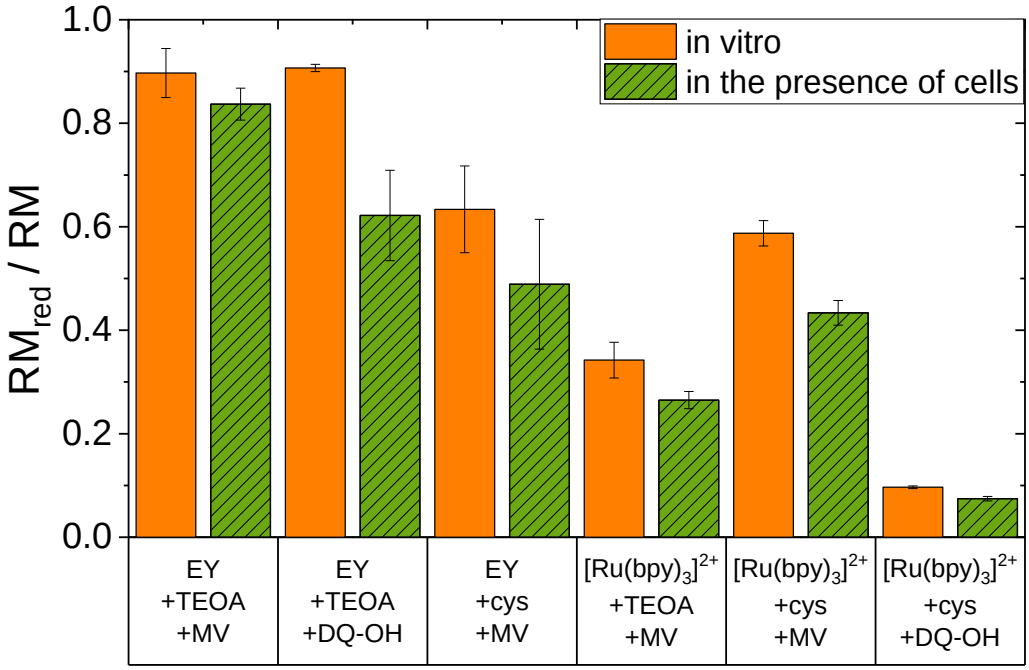

Figure S.I. 26. **Ratio of RM_{red} over total amount of RM upon continuous illumination**. Sample solutions contain 4 µM PS, 20 µM MV or 25 µM DQ-OH, and 100 mM SED in PBS solution (pH 7.5 for TEOA samples, or 6.5 for cysteine samples), in the absence (orange) or presence (green) of fresh *Cr*HydA1 containing *E. coli* cells (OD_{600} = 0.2); measurements are carried out under an inert gas atmosphere.

VII. Limiting factors

VII.1. Addition experiments

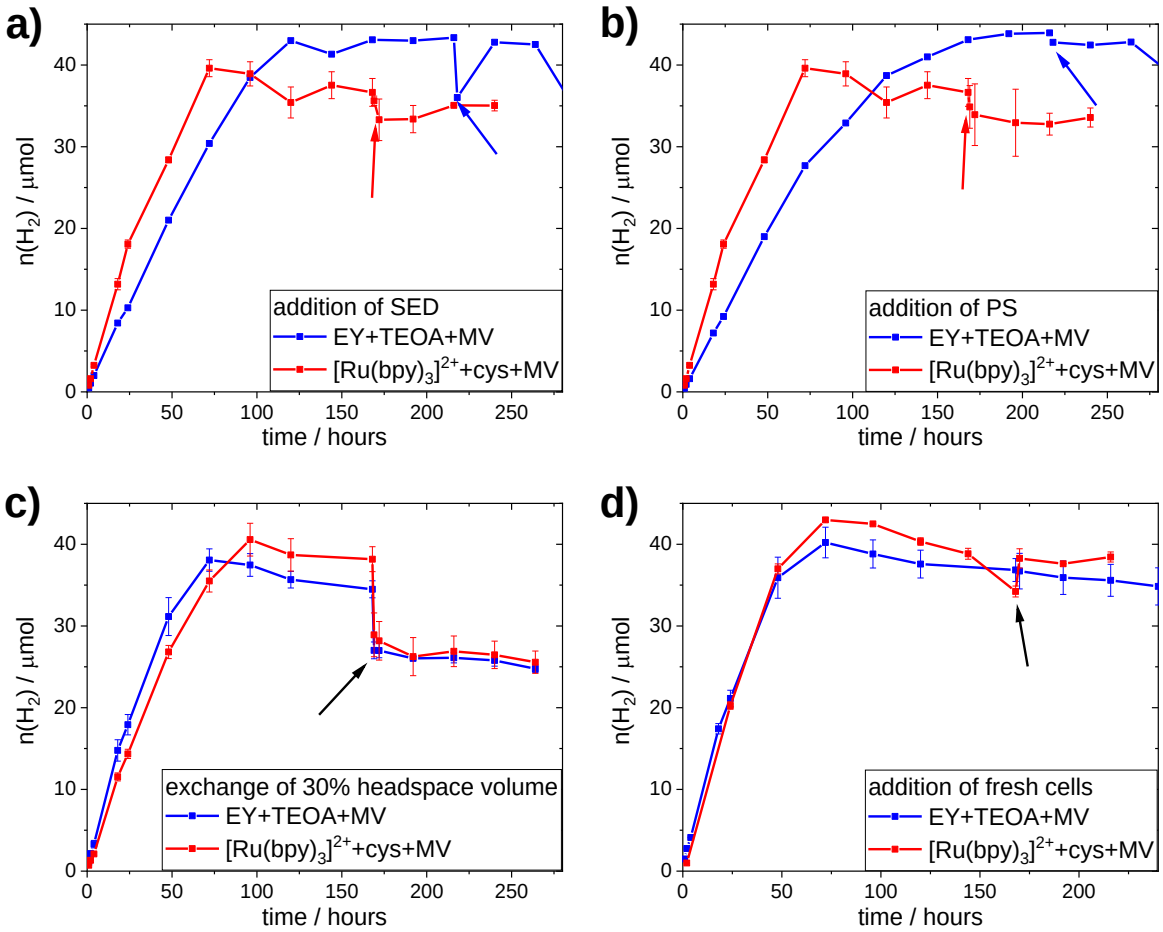

Figure S.I. 27. **Examination of Limiting Factors in Photocatalysis.** Samples contain 100 µM PS (EY or $[Ru(bpy)_3]^{2+}$), 1 mM MV, and 100 mM SED (TEOA at pH 7.5, blue traces; L-cysteine, pH 6.5, red traces; **a)** addition of 100 µL SED (TEOA or L-cysteine, 1 M); **b)** addition of 100 µL PS (EY or $[Ru(bpy)_3]^{2+}$, 1 mM); **c)** headspace gas exchange (30% v/v) against argon; **d)** addition of 100 µL fresh cells (OD_{600} = 50).

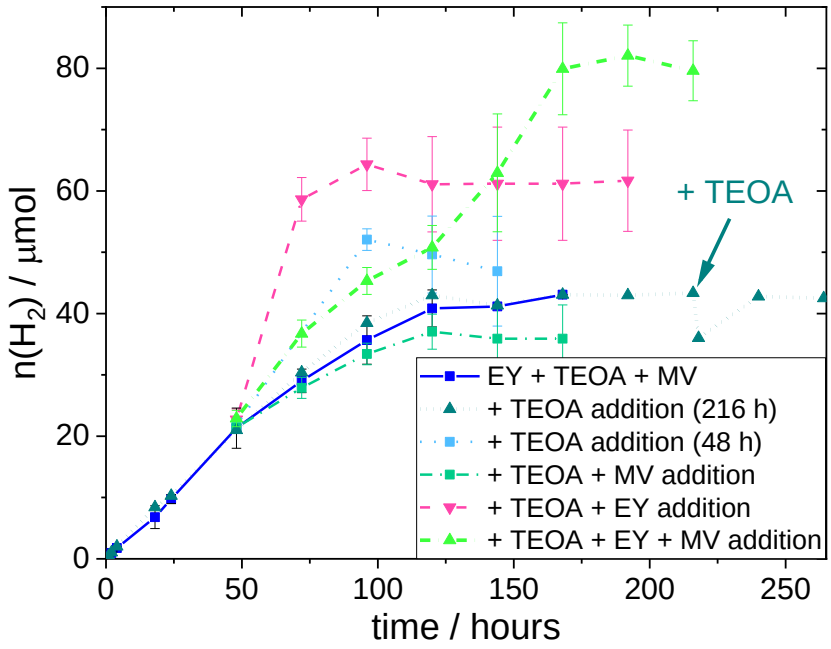

Figure S.I. 28. **Examination of Limiting Factors in Photocatalysis.** Starting samples contain 100 µM EY, 1 mM MV, and 100 mM TEOA at pH 7.5.

Similar to the $[Ru(bpy)_3]^{2+}$+L-cysteine+MV system discussed in the main manuscript, the maximum TON reached for EY+TEOA+MV systems is close to the expected maximum amount of hydrogen. However, TEOA is considered a two-electron donor[18], which should allow for much higher TON.

Addition of TEOA after the H_2 plateau is reached does not lead to a reactivation of H_2 production, similarly to the $[Ru(bpy)_3]^{2+}$+L-cysteine+MV system. However, even TEOA addition before the plateau is reached as well as starting with a higher TEOA concentration (see Figure 2c, main manuscript) does not lead to substantially higher TON. We have stated previously that decomposition of EY_{red} competes with the electron transfer to an acceptor.[5] Hence, early addition or higher starting concentrations of TEOA could lead to more efficient EY reduction, which then decomposes rather than being re-oxidized efficiently. Indeed, addition of both EY and TEOA yields an increased TON, albeit not as high as expected, based on overall TEOA available. Only when all three components of the photosystem are added, i.e. EY, TEOA and MV, the hydrogen evolution yields TONs that match the doubling of TEOA in the system. This excludes the build-up of toxic or inhibiting by-products in the assay solution as a limiting factor. Yet, it is unclear how exactly the decompositions of the single components affect each other and what role the potential second electron coming from TEOA plays.

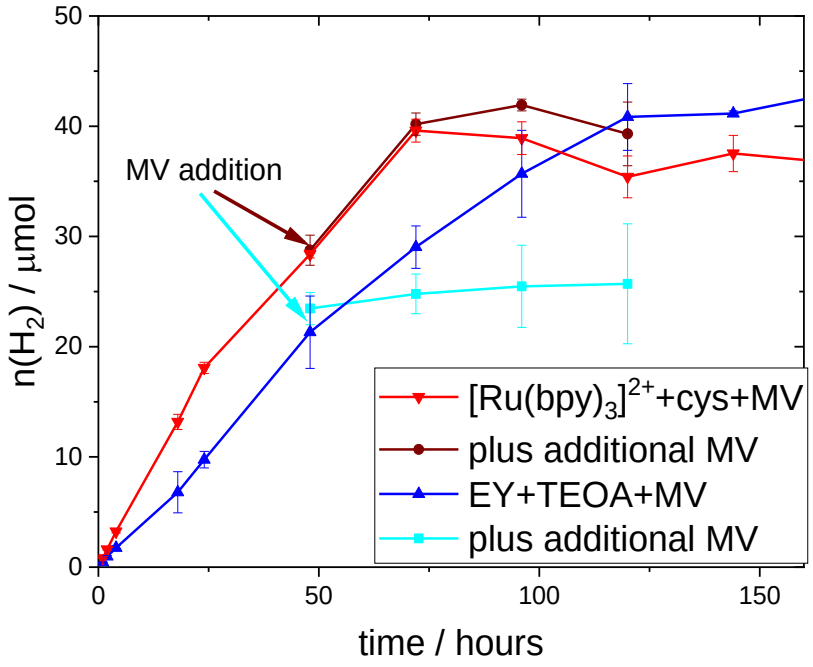

Figure S.I. 29. **Examination of Limiting Factors in Photocatalysis.** Samples contain 100 µM PS (EY or $[Ru(bpy)_3]^{2+}$), 1 mM MV, and 100 mM SED (TEOA at pH 7.5, blue traces; L-cysteine, pH 6.5, red traces; arrows indicate addition of 100 µL MV (10 mM). No improvement in the H_2-production was observable neither for the system working with EY+TEOA nor $[Ru(bpy)_3)]^{2+}$ + cys.

VII.2. Different [FeFe] hydrogenases

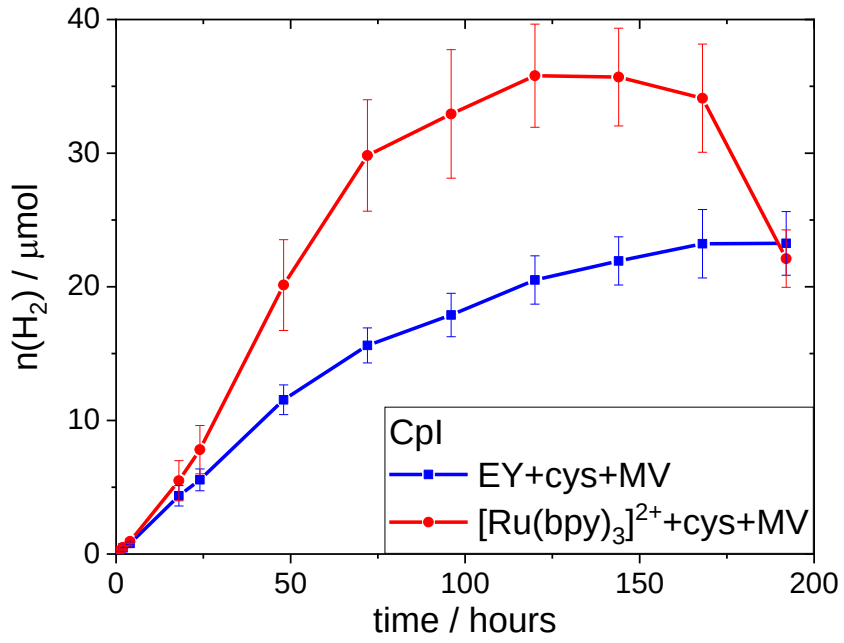

Figure S.I.30. **Photocatalytic H_2-Production Assay with CpI.** Assays were performed in 100 mM PBS-buffer (pH 6.5) supplemented with 100 mM L-cysteine, 100 µM PS (EY or $[Ru(bpy)_3]^{2+}$), and 1 mM MV, carried out under inert gas atmosphere at 30 °C under continuous illumination (4000 lx).

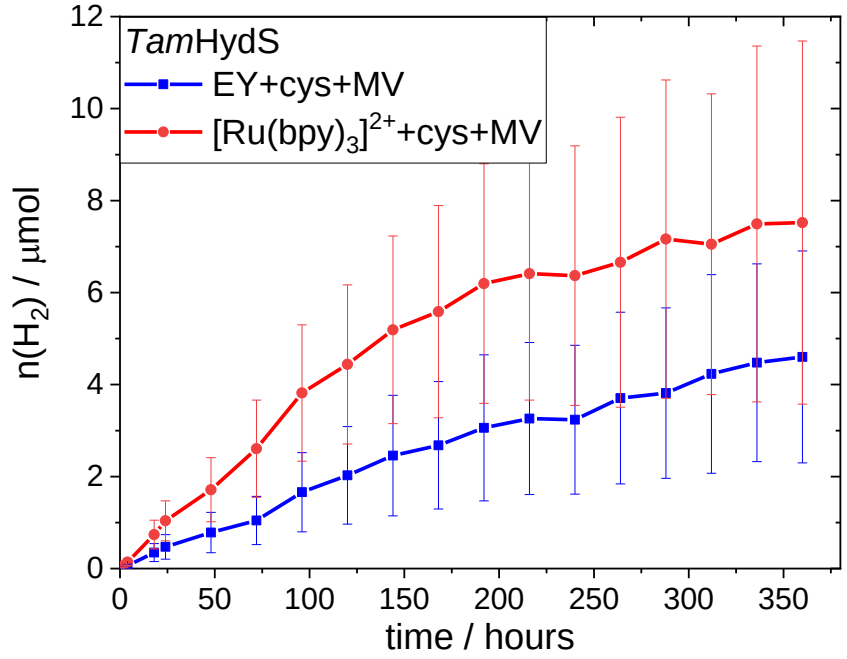

Figure S.I. 31. **Photocatalytic H_2-Production Assay with *Tam*HydS.** Assays were performed in 100 mM PBS-buffer (pH 6.5) supplemented with 100 mM L-cysteine, 100 µM PS (EY or $[Ru(bpy)_3]^{2+}$), and 1 mM MV, carried out under inert gas atmosphere at 30 °C under continuous illumination (4000 lx).

VIII. References

1. A. Le Cloirec, S. C. Davies, D. J. Evans, D. L. Hughes, C. J. Pickett, S. P. Best and S. Borg, *Chem. Comm.*, 1999, **22**, 2285-2286.
2. E. J. Lyon, I. P. Georgakaki, J. H. Reibenspies and M. Y. Darensbourg, *Angew. Chem, Int. Ed.*, 1999, **38**, 3178-3180.
3. M. Schmidt, S. M. Contakes and T. B. Rauchfuss, *J. Am. Chem. Soc.*, 1999, **121**, 9736-9737.
4. H. Li and T. B. Rauchfuss, *J. Am. Chem. Soc.*, 2002, **124**, 726-727.
5. M. T. Gamache, R. Charaf, L. Kurth, D. T. Filmon, M. Senger, N. Plumeré, L. Hammarström and G. Berggren, *ACS Catal.*, 2023, **13**, 9476-9486.
6. S. Hardt, S. Stapf, D. T. Filmon, J. A. Birrell, O. Rüdiger, V. Fourmond, C. Léger and N. Plumeré, *Nature Catalysis*, 2021, **4**, 251-258.
7. L. S. Meszaros, B. Nemeth, C. Esmieu, P. Ceccaldi and G. Berggren, *Angew Chem Int Ed*, 2018, **57**, 2596-2599.
8. K. A. Vincent, G. J. Tilley, N. C. Quammie, I. Streeter, B. K. Burgess, M. R. Cheesman and F. A. Armstrong, *Chem. Commun.*, 2003, 2590-2591.
9. A. Nilsen-Moe, A. Rosichini, S. D. Glover and L. Hammarström, *J. Am. Chem. Soc.*, 2022, **144**, 7308-7319.
10. K. Kalyanasundaram, J. Kiwi and M. Grätzel, *Helv. Chim. Acta*, 1978, **61**, 2720-2730.
11. M. Georgopoulos and M. Z. Hoffman, *J. Phys. Chem.*, 1991, **95**, 7717-7721.
12. K. Kalyanasundaram, *Coord. Chem. Rev.*, 1982, **46**, 159-244.
13. S. Tazuke, N. Kitamura and Y. Kawanishi, *Journal of Photochemistry*, 1985, **29**, 123-138.
14. C. R. Bock, T. J. Meyer and D. G. Whitten, *J. Am. Chem. Soc.*, 1975, **97**, 2909-2911.
15. R. C. Young, T. J. Meyer and D. G. Whitten, *J. Am. Chem. Soc.*, 1975, **97**, 4781-4782.
16. J. R. Darwent and K. Kalyanasundaram, *Journal of the Chemical Society, Faraday Transactions 2: Molecular and Chemical Physics*, 1981, **77**, 373-382.
17. I. Okura and N. Kim-Thuan, *J. Chem. Soc., Faraday Trans. 1*, 1981, **77**, 1411-1415.
18. Y. Pellegrin and F. Odobel, *Comptes Rendus Chimie*, 2017, **20**, 283-295.